Title: Application of a novel respirometric methodology to characterize mass transfer and activity of H_2S-oxidizing biofilms in biotrickling filter beds

Author: Wenceslao Bonilla-Blancas Mabel Mora Sergio Revah Juan Antonio Baeza Javier Lafuente Xavier Gamisans David Gabriel Armando González-Sánchez

PII: S1369-703X(15)00075-3
DOI: http://dx.doi.org/doi:10.1016/j.bej.2015.02.030
Reference: BEJ 6142

To appear in: *Biochemical Engineering Journal*

Received date: 24-5-2014
Revised date: 17-2-2015
Accepted date: 26-2-2015

Please cite this article as: Wenceslao Bonilla-Blancas, Mabel Mora, Sergio Revah, Juan Antonio Baeza, Javier Lafuente, Xavier Gamisans, David Gabriel, Armando González-Sánchez, Application of a novel respirometric methodology to characterize mass transfer and activity of H2S-oxidizing biofilms in biotrickling filter beds, Biochemical Engineering Journal http://dx.doi.org/10.1016/j.bej.2015.02.030

Application of a novel respirometric methodology to characterize mass transfer and activity of H_2S-oxidizing biofilms in biotrickling filter beds

Wenceslao Bonilla-Blancas[a,c,e], Mabel Mora[a], Sergio Revah[b], Juan Antonio Baeza[a], Javier Lafuente[a], Xavier Gamisans[d], David Gabriel[a], Armando González-Sánchez[c*]

[a]GENOCOV, Departament d'Enginyeria Química. Universitat Autònoma de Barcelona. Edifici Q. Campus de Bellaterra. 08193 Bellaterra, Barcelona, Spain.

[b]Departamento de Procesos y Tecnología, Universidad Autónoma Metropolitana Cuajimalpa, México D.F., Mexico.

[c]Instituto de Ingeniería, Universidad Nacional Autónoma de México, Ciudad Universitaria, México D.F., Mexico.

[d]Departament d'Enginyeria Minera i Recursos Naturals, Universitat Politècnica de Catalunya, Bases de Manresa 61-73, 08240 Manresa, Spain.

[e]Tecnológico de Estudios Superiores de Ecatepec, Ecatepec de Morelos, Mexico.

* Corresponding author: Coordination of Environmental Engineering, Building 5, 2nd Floor, Office 312, Engineering Institute UNAM, Circuito Escolar, Ciudad Universitaria, ZIP 04510 Mexico D.F., Mexico. Tel.: + (52) 55 56 23 36 00 x8711

agonzalezs@iingen.unam.mx

Highlights

- A novel respirometer design characterized the kinetics in H_2S-oxidizing biofilms
- H_2S biofiltration properties were evaluated from a sample of biotrickling filter bed
- Short-term respirometric assays (< 20 min) were performed
- A mathematical model of the biotrickling filter bed respirometry was developed
- The non-wetted biofilm fraction contributed 65% to the overall removal of H_2S

ABSTRACT

The elimination capacity of gaseous H_2S biofiltration can be limited either by mass transfer or bioreaction in the biofilm. Assessment of the biological activity of immobilized cells (biofilm) usually implies morphological and physiological changes during the adaptation of cells to respirometric devices operated as suspended cultures. In this study, respirometry of heterogeneous media is advised as a valuable technique for characterizing mass transport and biological activity of H_2S-oxidizing biofilms attached on two packing materials from operative biotrickling filters. Controlled flows of liquid and H_2S-containing air were recirculated through a closed heterogeneous respirometer allowing a more realistic estimation of the biofilm activity by the experimental evaluation of the oxygen uptake rate (OUR). Specific maximum OUR of 23.0 and 38.5 mmol O_2 (g biomass min)$^{-1}$ were obtained for Pall Rings and Polyurethane Foam, respectively. A mathematical model for the determination of kinetic-related parameters such as the maximum H_2S elimination capacity and morphological properties of biofilm (i.e. thickness and fraction of wetted area of packing bed) was developed and calibrated. With the set of parameters obtained, the external oxygen mass transport to the wetted biofilm was found to limit the global H_2S biofiltration capacity, whereas the non-wetted biofilm was the dominant route for the gaseous O_2 and H_2S mass transfer to the biofilm. Oxygen diffusion rate was the limiting step in the case of very active biofilms.

KEYWORDS

OUR; Hydrogen sulfide; heterogeneous respirometry; wetted/non-wetted biofilm; mathematical model; mass transfer.

1. INTRODUCTION

Hydrogen sulfide (H_2S) is a volatile inorganic compound commonly found in waste gas streams (e.g. biogas from landfills and wastewater treatment plants), with a typical composition ranging from 0.0002 % to 2.0% [1-2]. Biofilters (BF) and biotrickling filters (BTF) have been widely studied and applied by several research groups and companies to desulfurize polluted, odorous air or energetic gases such as biogas [3-4]. Therefore, the application of these technologies avoids the emission of harmful gases and odors, which cause human hazard risks and also corrosion damages on cogeneration engines in case of recovering energy from H_2S containing waste gases.

Several parameters can be monitored and controlled during waste gas biofiltration, such as inlet and outlet gaseous pollutant concentrations or flow rates, which allow calculating the overall removal efficiency. However, biodegradation kinetics are usually difficult to determine [5]. Respirometry consists on the measurement and interpretation of the biological oxygen consumption rate under well-defined experimental conditions and is a typical tool to assess the degradation activity of microbial cultures [6-7]. The performance of this assay has been traditionally used with suspended cells [8-9], namely Suspended Culture Respirometry (SCR), which implies biofilm destruction when it is applied to monitor biological activity of immobilized biomass. In SCR the original physiology of cells, as well as the mass transport phenomena occurring in the biofilm, are not considered which drives to an overestimated biological activity [10]. A realistic assessment of the biodegradation activity measured from a sample of colonized packed bed would allow improving the strategies to adequately operate and control biofilters.

Some adapted respirometric methodologies to study biodegradation kinetics of immobilized biomass have been already proposed. In this sense, preliminary studies have been performed towards the application of heterogeneous respirometry (HR) to characterize H_2S-oxidizing biofilms [5, 11]. However, in these methodologies the liquid and/or gas phases remained static [12-13], which do not simulate properly the dynamic nature of the flowing phases of a BF or BTF and, in consequence, altered the real biofilm conditions during tests. The effect of external mass transfer resistance on the H_2S elimination seems to be significant for the performance of BFs and BTFs, and especially in aerobic systems where the mass transport of gaseous oxygen to the biofilm could limit the global process [14]. Instead, the HR is a novel methodology based on the measurement of the biological activity of immobilized biomass with a minimum handling and damaging of the biofilm associated. HR also reproduces the dynamic conditions of the flowing phases. In addition, in the abovementioned studies only the pollutant concentration in the gas-phase has been monitored [15], while the oxygen concentration in the gas phase was not analyzed. The latter is a critical variable that defines the H_2S biological oxidation. Overall, the HR technique has not been extensively applied yet and requires further experimental and modeling research in order to be improved.

Thus, the aim of this work was to apply, assess and improve the HR methodology to characterize H_2S-oxidizing activity and mass transport phenomena of specialized biofilms grown on packed beds of desulfurizing BTFs. Complementary, a mathematical model is developed and calibrated to describe the process and the intrinsic oxygen uptake rates (OUR) induced by the oxidation of H_2S in the biofilm. The mathematical model considers both wetted and non-wetted biofilm surfaces of the packing material. Experimental data of oxygen profiles in the gas and the liquid phase together with the application of the mathematical model allowed

estimating the maximum H_2S elimination capacity of the packing materials. Although no experimental data was available from inside the biofilm, the model was used to theoretically identify and assess the potential limiting steps in H_2S bio-oxidation.

2. MATERIALS AND METHODS

2.1. Heterogeneous respirometer setup

The experimental system consisted of a transparent PVC cylindrical BTF, with an internal diameter of 0.06 m and a height of 0.50 m. The packed bed height filled with random packing was 0.26 m (a working volume of 0.73 L). In Fig. 1 a schematic of the HR is presented. During respirometric assays the liquid phase was continuously recirculated at a flow rate of $2.25 \cdot 10^{-2}$ $m^3\ h^{-1}$ with a peristaltic pump (77200-12, Cole Parmer, USA) while the gas phase was counter-currently recirculated with a gas compressor (Model 3112, Boxer, England) at 0.09 $m^3\ h^{-1}$.

Here Figure 1.

The HR was provided with an oxygen gas analyzer (SIDOR module OXOR-P, SICK, Germany) and also with a galvanic dissolved oxygen sensor (CellOx 325, WTW, Germany) connected to a bench top meter (Inolab Terminal level 3, WTW, Germany) to monitor the oxygen concentration in each phase. The pH was monitored in-situ (Sentix 20,WTW, Germany) and accurately controlled at 7.0± 0.1 by a high precision two-channel micro-burette (Multi burette 2S, Crison, USA) by 1M HCl and 1M NaOH addition. Sensors data were continuously recorded in a personal computer with software developed for process monitoring

and control with NI LabWindows CVI. Temperature was not directly controlled in the HR. Instead, room temperature was kept constant at 21ºC.

2.2. H_2S-oxidizing immobilized biomass

Two desulfurizing BTFs with different packing material, polyurethane foam cubes (EDT, Eckenhaid-Eckental, Germany) and stainless steel pall rings (KEVINCPP, Mumbai, India), namely PUF and PR, respectively, were used in this study (Table SM1, Supplementary Material). The BTFs were inoculated with activated sludge from a municipal wastewater treatment plant to obtain an enriched neutrophilic H_2S-oxidizing consortium. Initially, the inoculum was circulated through the packing material during 8h without liquid renewal and with a counter-current aeration flow of 0.03 $m^3 \cdot h^{-1}$. Afterwards, the BTF was fed during 2 months with a constant H_2S inlet concentration of 300 ppm_v while setting the empty bed residence time (EBRT) to 30 s (48 g S m^{-3} h^{-1}). The pH was monitored and automatically controlled to 7.0. The composition of the mineral medium used to grow up the immobilized culture contained (g L^{-1}): NH_4Cl, (1); KH_2PO_4, (0.12); K_2HPO_4, (0.15); $CaCl_2$, (0.02); $MgSO_4 \cdot 7H_2O$, (0.2); and trace elements, 1 mL L^{-1} [4]. Additionally, bicarbonate was added as the microbial carbon source to the mineral medium (3.5 g L^{-1} $NaHCO_3$).

2.3. Experimental approach of the heterogeneous respirometry

Abiotic and biotic experiments were performed to characterize the mass transfer phenomena and the H_2S-oxidizing activity of the biofilm. First, several abiotic assays were performed at different gas and liquid linear velocities with two types of packing material (PUF and PR) to estimate the overall volumetric mass transfer coefficient ($K_L a_{g\text{-}l}$) corresponding to oxygen. The procedure to obtain the experimental data was applied as follows. The BTF was filled with

sterilized packing material followed by the addition of mineral medium (126 mL). The gas and liquid phases were counter-currently circulated while all oxygen was stripped out from the HR by feeding nitrogen gas at a flow of 0.03 $m^3 \cdot h^{-1}$. Once the oxygen was absent, a controlled air flow (0.03 $m^3 \cdot h^{-1}$) was fed to the HR generating different time-depended oxygen concentration profiles in both phases. Different velocities for gas (43.4; 57.8; 77.1; 101.2 m h^{-1}) and liquid (6.9; 8.3; 10.8 m h^{-1}, respectively) were applied to assess the mass transfer phenomena in the BTF. The liquid was assumed to be pure water due to the low salt content. Then, no ionic effects were considered over oxygen transfer. Gaseous and dissolved oxygen profiles arising from the abiotic assays were used to estimate the corresponding $K_L a_{g\text{-}l}$.

For the biotic assays, colonized packing material was withdrawn from the BTFs packed with PUF and PR, respectively. The experimental test started with the addition of 126 mL of mineral medium into the HR, which was continuously recirculated and aerated for some hours in order to stabilize the biofilm and to allow exhausting the bioavailable substrates that could have accumulated in the biofilm during the BTF operation (mainly H_2S). Afterwards, the HR was closed and, while both phases were continuously recirculated, a pulse of gaseous pure H_2S (10 mL) was immediately injected in the gas phase to attain computed equilibrium concentrations of 0.62 mmol L^{-1} (19.8 g m^{-3}) and 0.63 % (vol) in the liquid and gas phases, respectively. The measurement of the equilibrium concentration into the liquid phase was theoretically calculated using the corresponding Henry's constant for H_2S (He=0.41 [16]). Gas and liquid phases were circulated at linear velocities of 101.2 and 10.8 m h^{-1}, respectively, and the oxygen concentration evolution was continuously monitored in both phases. The abiotic and biotic assays were performed by triplicate and once (H_2S consecutive additions affected the biofilm physiology) respectively. Experimental conditions in terms of substrate, electron acceptor and biomass concentrations must be those that allow *OUR* to be sensitive enough to produce a short

test (to avoid large biomass growth) with reduced uncertainty due to noise of measurements. Large substrate concentrations in the gas phase are important since produce significant variations of oxygen both in the gas and in the liquid phase. The latter is particularly important when activity tests are combined with modeling to determine model parameters or to predict system performance.

2.4. Experimental determinations in the packed bed

The amount of biomass attached to the packing support was quantified as follows [17]. Once the corresponding assay was finished, the liquid pump was stopped and the packing material was immediately weighted (W_1). After draining the liquid for a period of 30 minutes, the support was weighted again (W_2). The weight difference between W_2 and W_1 was used to determine the static hold-up which, together with the dynamic hold-up, was used to estimate the volume fraction occupied by the liquid (ε_l^{Bed}). Once drained, the packing material was carefully squeezed and/or shaken to withdraw all the biofilm and suspend it in a known amount of water. The clean packing was dried for 12 hours in an oven at 50 °C to determine the weight of the support (W_3). The suspended biomass was later centrifuged at 5000 rpm for 10 minutes and the supernatant was discarded to determine the weight of wet biomass (W_4). The volume fraction occupied by the biofilm (ε_b^{Bed}) was calculated dividing W_4 by the product of wet biofilm density times the volume of the packing material tested. A wet biofilm density of 1.11 g mL^{-1} reported by Hugler et al. [18] for a similar biofilm was used to calculate ε_b^{Bed}. Finally, the wet biomass was dried for 12 hours at 50 °C to determine the dry weight of the biomass (W_5). The volume fraction occupied by the gas (ε_g^{Bed}) in the packed bed was also determined

taking into account the space occupied by the abovementioned fractions of the packed bed, including the empty bed fraction of the packing material reported by the manufacturer (see Table 1).

2.5. Mathematical model development

Mass balances for oxygen and H_2S in the gas, liquid and biofilm phases of the HR were stated in Eqs. (1-6) based on the modeling approach by González-Sánchez et al. [19]. Due to bench size and the batch operating mode of the HR, an ideally mixed regime was assumed for both bulk phases. The reaction was considered to occur entirely in the biofilm since there was no suspended biomass in the liquid phase either at the beginning or at the end of the assays. The reaction considered in this study is a biological reaction being the catalyzer the biomass itself. Free volumes of gas in the upper and lower sections of the HR and the liquid reservoir (see Fig. 1) were also considered in mass balances. As a particular assumption associated with the operation mode and size of the experimental system, no axial concentration gradients were considered due to the continuous recirculation of gas and liquid phases. The mechanism proposed for H_2S removal in the BTF is shown in Fig. 2. Both wetted and non-wetted portions of the biofilm were included in the model. As a common assumption often made in biofiltration modeling, mass transfer resistance in the gas boundary layer over the wetted and non-wetted biofilm was assumed negligible. More detailed model assumptions can be found elsewhere [5, 20].

Here Figure 2.

2.5.1 Mass balance for the gas phase.

In the packed bed

$$\frac{dC_{g,i}^{Bed}}{dt} = \frac{Q_g}{V_{Bed} \cdot \varepsilon_g^{Bed}} \cdot \left(C_{g,i}^{Free} - C_{g,i}^{Bed} \right) - \frac{K_L \cdot a_{g-l}}{\varepsilon_g^{Bed}} \cdot \left(\frac{C_{g,i}^{Bed}}{He_i} - C_{l,i}^{Bed} \right) - \frac{K_B \cdot a_{g-b}}{\varepsilon_g^{Bed}} \cdot \left(\frac{C_{g,i}^{Bed}}{He_i} - C_{b-NW,i} \right) \quad (1)$$

with initial condition:

$t = 0 \quad C_{g,i}^{Bed} = C_{g,i}^{0}$

In the gaseous reservoir

$$\frac{dC_{g,i}^{Free}}{dt} = \frac{Q_g}{V_{g,i}^{Free}} \cdot \left(C_{g,i}^{Bed} - C_{g,i}^{Free} \right) \quad (2)$$

with initial condition:

$t = 0 \quad C_{g,i}^{Free} = C_{g,i}^{0}$

The subscript *i* refers to oxygen or H_2S, the two different gaseous compounds considered in the mass balance.

2.5.2. Mass balance for the liquid phase.

In the packed bed

$$\frac{dC_{l,i}^{Bed}}{dt} = \frac{Q_l}{V_l^{Bed}} \cdot \left(C_{l,i}^{Res} - C_{l,i}^{Bed} \right) + \frac{K_L a_{g-l}}{\varepsilon_l^{Bed}} \left(\frac{C_{g,i}^{Bed}}{He_i} - C_{l,i}^{Bed} \right) - \frac{K_B \cdot a_{l-b}}{\varepsilon_l^{Bed}} \cdot \left(C_{l,i}^{Bed} - C_{b,i} \right) \quad (3)$$

with initial condition:

$t = 0 \quad C_{l,i}^{Bed} = C_{l,i}^{0}$

In the liquid reservoir

$$\frac{dC_{l,i}^{Res}}{dt} = \frac{Q_l}{V_l^{Res}} \cdot \left(C_{l,i}^{Bed} - C_{l,i}^{Res} \right) \quad (4)$$

with initial condition:

$t = 0 \quad C_{l,i}^{\mathrm{Res}} = C_{l,i}^{0}$

2.5.3. Mass balance for the biofilm

Wetted biofilm

$$\frac{\partial C_{b,i}}{\partial t} = D_{eff,i} \frac{\partial^2 C_{b,i}}{\partial x^2} - r_{b,i} - OUR_{end} \quad (5)$$

with boundary conditions:

$t = 0; C_{b,i} = C_{b,i}^{0}$

$x = 0; \quad C_{b,i} = C_{l,i}$

$x = \delta; \quad \frac{\partial C_{b,i}}{\partial x} = 0$

Non-wetted biofilm

$$\frac{\partial C_{b-NW,i}}{\partial t} = D_{eff,i} \frac{\partial^2 C_{b-NW,i}}{\partial x^2} - r_{b-NW,i} - OUR_{end} \quad (6)$$

with boundary conditions:

$t = 0; \quad C_{b-NW,i} = C_{b-NW,i}^{0}$

$x = 0; \quad C_{b-NW,i} = \frac{C_{g,i}}{He_i}$

$x = \delta; \quad \frac{\partial C_{b-NW,i}}{\partial x} = 0$

$C_{g,i}^{Bed}, C_{l,i}^{Bed}$ $C_{b,i}$ and $C_{b-NW,i}$ are the concentrations of component *i* in the bulk gas phase, bulk liquid phase, biofilm and non-wetted biofilm, respectively (g m^{-3}); $C_{g,i}^{Free}$, $C_{l,i}^{\mathrm{Res}}$ are the concentrations of component *i* in the free gas volume and in the liquid reservoir tank respectively (g m^{-3}); He_i is the gas/liquid partition coefficient of component *i* (dimensionless); a, a_{g-l}, a_{l-b}, a_{g-b} (see Eqs. 8-10) represent the specific surface area per volume unit of packed bed, gas-liquid specific contact area, liquid-biofilm specific contact area and gas-biofilm specific contact area, respectively (m^2 m^{-3}); $D_{eff,i}$ is the diffusion coefficient of component *i* in the biofilm (m^2 h^{-1});

$r_{b,i}$, $r_{b-NW,i}$ are the consumption rates of component *i* in the wetted biofilm and in the non-wetted biofilm respectively (g m^{-3} h^{-1}); δ is the biofilm thickness (m).

2.5.4. Model solution

N is the total number of layers of the discretized biofilm thickness for the numerical resolution of the mathematical model. According to Eq. (7), K_B is the external mass transfer coefficient from external bulk phase to biofilm. The surface fraction of the packing material covered by biofilm (β) was estimated according to Eq. (11).

$$K_B = \frac{D_{eff,i} \cdot N}{\delta} \tag{7}$$

$$a_{g-l} = a \cdot \alpha \tag{8}$$

$$a_{l-b} = \beta \cdot a_{g-l} \tag{9}$$

$$a_{g-b} = \left(a - a_{g-l}\right) \cdot \beta \tag{10}$$

$$\beta = \frac{\varepsilon_b^{bed}}{a \cdot \delta} \tag{11}$$

The set of partial differential equations was discretized in space along the biofilm thickness. Six points were used along the biofilm thickness. The resulting set of ordinary differential equations was solved using a Rosenbrock (stiff) integration method with Berkeley Madonna 8.3.18.

2.5.5. Microbial kinetics

The OUR within the biofilm was described by a double Monod-Haldane type kinetic expression depending on dissolved oxygen and dissolved H_2S concentrations inside the biofilm (Eqs. 12 and 13). The H_2S uptake rate was computed from Eqs. (14) and (15) as a function of the stoichiometric yield of sulfide oxidation.

Wetted biofilm:

$$r_{b,\cdot O_2} = OUR_{\max} \cdot \left(\frac{C_{b,O_2}}{C_{b,O_2} + K_{S,O_2}} \right) \left(\frac{C_{b,H_2S}}{K_{S,H_2S} + C_{b,H_2S} + \frac{(C_{b,H_2S})^2}{k_I}} \right) \quad (12)$$

Non-wetted-biofilm:

$$r_{b-NW,\cdot O_2} = OUR_{\max} \cdot \left(\frac{C_{b-NW,O_2}}{C_{b-NW,O_2} + K_{S,O_2}} \right) \left(\frac{C_{b-NW,H_2S}}{K_{S,H_2S} + C_{b-NW,H_2S} + \frac{(C_{b-NW,H_2S})^2}{k_I}} \right) \quad (13)$$

While:

$$r_{b,H_2S} = \frac{r_{b,O_2}}{Y_{O_2/H_2S}} \quad (14)$$

$$r_{b-NW,H_2S} = \frac{r_{b-NW,O_2}}{Y_{O_2/H_2S}} \quad (15)$$

2.5.6. Stoichiometry of H_2S oxidation

Recent reports [15] stated that elemental sulfur or sulfate production occur depending on the molar ratio of dissolved oxygen and sulfide species in the biofilm, namely $[O_2]/[H_2S]$ ratio. At molar ratios $[O_2]/[H_2S] \leq 1.0$ H_2S oxidation occurs through Eq. (16) at a stoichiometric yield Y_{O_2/H_2S} = 0.5 while Eq. (17) predominates at a stoichiometric yield Y_{O_2/H_2S} = 2.0 when the molar ratio $[O_2]/[H_2S] > 1.0$. During modeling of respirometric assays, the molar ratio $[O_2]/[H_2S]$ in

the biofilm was evaluated at each integration step of the differential equations set in order to predict the fate of H_2S oxidation. A step switch function was programmed to use the corresponding molar yield.

$$H_2S + 0.5O_2 \rightarrow S^0 + H_2O \quad (16)$$

$$H_2S + 2O_2 \rightarrow SO_4^{2-} + 2H^+ \quad (17)$$

Furthermore, the calibrated model was used to predict the transient H_2S elimination capacity of the biotrickling filter bed (g H_2S m^{-3} bed h^{-1}) considering the fate of H_2S as well as the contribution of wetted and non-wetted biofilm to H_2S elimination according to Eq. (18).

$$EC_{H_2S} = \left[(r_{b,O_2} \cdot a_{l-b}) + (r_{b-NW,O_2} \cdot a_{g-b}) \right] \cdot \frac{\delta}{0.94 \cdot Y_{O_2/H_2S}} \quad (18)$$

Where 0.94 corresponds to a conversion factor from molar to mass units (mol O_2 mol^{-1} H_2S to g O_2 g^{-1} H_2S).

2.6. Model parameters estimation

Physical and some biokinetic parameters included in the model were either experimentally determined or taken from literature while others were obtained from the packing materials manufacturers (Table 1).

HereTable 1.

The experimental gaseous and dissolved oxygen concentration profiles generated from the respective respirometric tests were used to calibrate the mathematical model described above. Only three biokinetic (OUR_{max}, $Ks_{,H2S}$ *and* $Ki_{,H2S}$) and one morphological parameters (biofilm thickness δ) were determined by fitting the experimental data. Parameters estimation was performed following the least square method by minimizing the quadratic error between model predictions and measured gaseous and dissolved oxygen concentrations. Model simulations and parameters estimation were performed with Berkeley Madonna 8.3.18 software. A statistical analysis based on paired t-student tests at a 5% level of significance were performed for dissolved oxygen and oxygen gas in both packing materials in order to quantify the agreement between results predicted by the model with the optimized kinetic parameters and experimental data.

3. RESULTS

3.1. Abiotic tests

Fig. 3 shows the $K_La_{g\text{-}l}$ as a function of the hydrodynamic conditions for both packing materials. Results indicated that the gas velocity had a larger impact on $K_La_{g\text{-}l}$ compared to the impact of increasing the liquid velocity for both packing materials. Here the unexpected effect of the increase of gas velocity on the $K_La_{g\text{-}l}$ can be due to the excessive mixing of liquid, which caused a sensible reduction of the resistance to the mass transport in the liquid side. Also, slightly higher mass transfer coefficients were found for PR compared to PUF under all conditions tested. Hydrodynamic conditions that lead to a $K_La_{g\text{-}l}$ of around 20 h^{-1} (gas and

liquid flow rates of 43.4 m h^{-1} and 10.8 m h^{-1}, respectively) were selected as convenient for biofiltration operation according to Kim and Deshusses [5]. Therefore, such conditions were set for subsequent biotic tests.

Here Figure 3.

3.2. Model calibration in biotic tests

Fig. 4 shows the oxygen concentration changes in gas and liquid phases induced due to the biological H_2S oxidation in the corresponding packed bed tested. The total biofilm mass experimentally assessed on PR and PUF was 2.1 and 7.0 g VSS, respectively. Solid lines show the HR model predictions after optimization of OUR_{max}, δ, $K_{s,H2S}$ and $K_{i,H2S}$ for both packing materials. Overall, a good agreement was found for the oxygen profiles in the gas phase for both packing materials. Also, the dissolved oxygen concentration predicted for the PR packing was satisfactory (Fig.4A) while a slight overestimation of the oxygen consumption was found for PUF towards the end of the test. The t-Student tests executed for all variables in Fig. 4 ($C_{l,O2}$ and $C_{g,O2}$) yielded absolute values in between the two t-test tails at a 5% level of significance indicating that the differences between dissolved oxygen and oxygen gas measured experimentally and those predicted by the model were not statistically significant in the studied period for PUF.

Here Figure 4.

The fitted parameters as well as other relevant estimates calculated from model estimates are shown in Table 2. At the trickling rate tested (10.8 m h^{-1}), the fraction of biofilm covered by water (assuming to be proportional to α) was much smaller than that directly exposed to the gas for both packing materials. Even if the thickness of the biofilm on PUF was more than half that of the PR, the surface of packing covered by biofilm (β), the area of biofilm directly exposed to the gas phase ($a_{g\text{-}b}$) as well as the OUR_{max} were significantly larger for the PUF packing compared to those for the PR. Results in Table 2 indicate that a combination of several factors lead to find a larger H_2S elimination capacity for the PUF packing. The external oxygen mass transfer coefficients K_L and K_B would explain such differences as discussed later.

HereTable 2.

Similarly, the overall capacity for H_2S degradation must consider not only mass transport but also the biological activity inside the biofilm. Table 2 also shows the maximum *EC* estimated by the model corresponding to the maximum activity along the biotic test for each packing material (Fig. 5). The experimental *EC* during the whole respirometric assay for both type kinetic assays was around 52 g H_2S m^{-3} h^{-1} which was much lower than the maximum *EC* predicted by the model. Such a difference can be explained by the fact that the maximum *EC* is computed at a specific time under favorable oxygen and H_2S concentrations in the biofilm, while on the other the conditions during the respective respirometric assay changed from

nearby inhibitory to limiting H_2S concentrations, this resulted in an averaged *EC* value that underestimates the potential *EC* of the colonized sampled bed

Oppositely to that of PR, the *EC* estimated for PUF indicated that H_2S was almost depleted at the end of the test. In the first 2 minutes an initial lag phase was found for both packing materials. As commonly found in respirometric tests performed in SCR, such behavior was related to the wake-up time needed by microorganisms for adapting to the test conditions after the endogenous phase. Also, model predictions based on the contribution of the wetted and non-wetted fraction as calculated by Eq. (18) indicated that the non-wetted biofilm fraction in both packing materials contributed in average around 65% to the *EC* observed (Fig. 5).

Here Figure 5.

3.3. Assessment of the rate controlling step

Although no experimental data of the concentrations of the species inside the biofilm was available at the time of the study, the calibrated HR model was used to predict the theoretical profiles of the electron donor and acceptor inside the biofilm at two particular times of the respirometry. First, at the time of reaching the maximum H_2S elimination capacity EC_{max}, namely t_{max}, and secondly at the end of the test, namely t_{end} (Fig. 5). Fig. 6 shows the predicted concentrations of H_2S and dissolved oxygen inside of the wetted and non- wetted biofilm for both packing materials at both t_{max} and t_{end}. In Fig. 6A and 6B for the wetted biofilm a similar behavior can be observed for both colonized packed beds independently of the time at which profiles were assessed. Almost the whole biofilm was active in both cases except in the inner

layers of the PUF biofilm at t_{end} (Fig. 6B) since H_2S had been almost completely consumed at the end of the test. Except in the latter case, no substrate limitation occurred in the wetted fractions of the biofilm. For PUF at t_{max} (Fig. 6D), the H_2S elimination capacity in the non-wetted biofilm was limited by the diffusion of oxygen through the biofilm. The inner layers turned out to be inactive for both packing materials.

Here Figure 6.

Since different H_2S and O_2 concentrations in the biofilm existed along time and biofilm depth, the H_2S elimination rates and its controlling factor depended on the molar $[O_2]/[H_2S]$ ratio which, in turn, defined the products of H_2S oxidation. Fig. 7 shows the molar $[O_2]/[H_2S]$ ratio through the biofilm thickness computed at the same time than those in Fig. 6. According to Eqs. (14) and (15), a combination of elemental sulfur and sulfate were being produced in both packing materials.

Here Figure 7.

4. DISCUSSION

The use of bacterial biofilm as catalyst for the desulfurization of biogas in biotrickling filters is highly convenient in terms of its easy design and operation, but difficult to keep good performance if not enough knowledge about the complex phenomena occurring in the biofiltration process is available. Oppositely to SCR, HR can mimic the hydrodynamic

conditions found in a BTF allowing the estimation of the intrinsic biological activity of the biofilm by inducing comparative boundary layer properties of the mobile phases. Besides, the HR methodology described in this work considers and quantifies phenomena such as the partial wetting of both the packing and biofilm that occur in real biotrickling filters.

Abiotic tests performed for the packing materials under study indicated that both packing materials showed similar performance and values for the oxygen $K_L a_{g\text{-}l}$. Kim and Deshusses [21] suggested a proportional relationship of the liquid linear velocities to the $K_L a$ of oxygen, which was confirmed in this work. Despite of the lower specific surface area of PR compared to PUF, slightly higher $K_L a_{g\text{-}l}$ values for PR were found. Characterization of PUF in several works has shown that the reticulate structure of PUF provides a large accumulation of water in packed beds in the form of water droplets [22]. Both results suggest that such water accumulation in PUF does not necessarily improve G-L mass transfer if water is not well distributed as a thin layer over the surface of the packing material. In fact, Table 2 shows that α, the fraction of the packing surface covered with water, was estimated to be similar for PR and PUF [5]. Then, the larger bulk porosity of PUF does not correspond to a better water trickling since a fraction of the water accumulated inside the foam may not be accessible for G-L mass transfer. Therefore, water and biofilm distribution over the surface of both packing materials had a large impact in the performance of the system as shown in biotic tests.

In biotic assays, t-Student test showed that model predictions were in good agreement with experimental results indicating that mass transport and biological kinetics were satisfactorily included in the HR model. Biofilm concentration profiles presented in Fig. 6 indicated that the wetted biofilm had a limited G-L oxygen transport compared to that of H_2S, i.e. solubility, which could have conditioned the bioreaction rate at first layers of biofilm, due to slightly

larger accumulation of H_2S at t_{max} in the wetted biofilm than the accounted for the non-wetted biofilm. According to González-Sánchez et al. [23], at concentrations >15 mM H_2S a partial substrate inhibition of the H_2S degradation rate could occur, explaining why almost all wetted biofilm was active but not fast enough. The H_2S external transport was not relevant here because of its much higher solubility (He=0.41) compared to that of oxygen (He=32) under standard conditions. In the non-wetted biofilm, where no external mass transport resistance existed, bioreaction rates were maximized in the external layers but minimized in the deeper layers of the biofilm. This observation previously find by others [24-25] indicates that both oxygen and H_2S diffusion rates through biofilm limited the activity of the biofilm.

Results also allowed calculating the contribution of the wetted and non-wetted fractions to the total flux of H_2S and O_2 to the biofilm. Since wetted surfaces ($a_{l\text{-}b}$) were lower for PR and PUF compared to the non-wetted surface ($a_{g\text{-}b}$), the contribution of the G-L flux and that of the G-B flux was significantly different for both packing materials. According to the mass transport terms in Eq. (1), the oxygen G-B flux was 0.53 g O_2 m^{-2} h^{-1}, while the corresponding G-L flux was 0.23 g O_2 m^{-2} h^{-1} for PUF. Similarly, gas fluxes of 0.41 and 0.05 g O_2 m^{-2} h^{-1} for G-B and G-L fluxes, respectively, were found for PR. Nevertheless, the H_2S elimination capacity predicted by the model (Eq. (18)), scrutinized in average that around 65% of the H_2S eliminated in the BTF was due to the non-wetted biofilm for both packing materials tested, similar trend was reported by Li et al. [26]. However, a different behavior to the oxygen fluxes was computed for H_2S, resulting in a G-L flux slightly higher than the G-B flux, which can be explained in terms of the gradient concentrations conditioning the mass fluxes (Eq. (1)). In the case of H_2S, these concentration gradients were similar either for G-L and G-B interphases, which indicated that no external mass transfer limitation of H_2S occurred, mainly due to its

much higher solubility than that of oxygen. Here the H_2S solubility can be sensibly enhanced by its absorption in aqueous solutions at pH>7 [27]. In addition, experimental results about biomass density indicated that the biofilm amount on the PUF was twice larger than that on PR, so different distribution in the bed leads to key consequences in terms of H_2S removal. In the case of PUF, a thinner biofilm, as well as a larger surface colonized by biofilm than that obtained with PR lead to a PUF biofilm much more active (4 times compared with PR taking as reference the EC_{max}) with a larger capacity for oxygen consumption and concomitant H_2S degradation. Overall, results are consistent with the common experimental evidence that a higher water hold-up in biotrickling filters leads to reduced *EC* and removal efficiencies [21, 28-30] and especially for poorly soluble compounds as O_2. In any case, results presented herein become in an interesting theoretical framework in the sense that previous models that considered wetted and non-wetted biofilms either took into account only the absorption of pollutant in the G-L interphase [24-25] or did not analyze the contribution G-L and G-B mass fluxes [5]. Results herein point out that both G-B as well as G-L transfer fluxes must be considered and analyzed separately depending on the solubility of each compound.

The model predicted that maximum *EC* for H_2S occurred close to or under oxygen limiting conditions in both wetted and non-wetted biofilms. Reported H_2S elimination capacities are between 50 to 400 g H_2S m^{-3} h^{-1} [5, 14, 31-32] for different BTFs packed with various materials and operated under similar conditions, which were in general lower than the predicted by the calibrated mathematical model. This fact shows that conventional BTFs could not be optimally operated, meaning that the biofilm has to be exposed to optimal H_2S concentrations (non-limiting and non-inhibiting) as well as non-limiting oxygen concentrations. These ideal conditions could be very difficult to reach, especially in full-scale BTFs, where probably a

large percentage of biofilm has low or no H_2S-oxidizing activity. As pointed out by other authors, the use of intensive devices for O_2 transport to the liquid phase, which is the main bottleneck when high loads of H_2S are removed, may help to improve the performance of BTFs [33].

Also, model predictions helped understanding the different instant by-products production from H_2S biological oxidation in a range of situations. Although at the end of the tests an oxygen excess condition was reached and, concomitantly, sulfate was the main product of H_2S oxidation (Fig. 7), elemental sulfur was the main product in almost all situations for PR. Elemental sulfur could be only produced in the inner layers of the non-wetted biofilm at t_{max} for PUF. The molar ratios $[O_2]/[H_2S]$ predicted inside of the biofilm indicate that maximum elimination capacities should be reached under oxygen limiting conditions in the first layers, but this means to overload the biofilm with H_2S. This could induce several performance risks, i.e. reaching inhibitory H_2S concentrations (>0.15 mM) [23] or clogging the biofilter bed by excessive formation and accumulation of elemental sulfur [34-36]. Instead, excess oxygen is desirable in terms of biofilter operation, but expensive because of the need to keep neutral pH (see Eq. (14)) as well as to promote adequate oxygen transfer if high loading rates of H_2S are treated [4]. Other factors not considered herein such as the reticulate structure of PUF must be also included in order to analyze the performance of different packing materials based on the HR. As an example, the larger biomass retention capacity of PUF may be counterproductive when elemental sulfur is produced in the bed.

Overall, experimental data of the gas and the liquid phases to both describe mass transfer and biological activity showed that dissolved oxygen and O_2 profiles allowed to assess the biological activity of a sample of packing material from a packed bed biological reactor and to

provide a theoretical benchmark to explain such behavior. It is worth mentioning that model predictions in terms of the concentrations of the species in the biofilm phase as well as several model parameters are influenced by the lack of experimental data from inside the biofilm phase. Data other than oxygen, which may include the fate of sulfide and its degradation subproducts, is warranted for improving the modeling approach proposed herein, even if data in such type of systems is difficult, even impossible in some cases, to obtain. Most modeling literature, dealing with biofilters and biotrickling filters, report only gas phase data [37-40] while almost no literature reports data inside biofilms since complex setups are needed and only few probes available. As an example, sulfur production or deposition, which would serve to better understand the H_2S oxidation cannot be measured directly. Elemental sulfur measurements are not reliable, even less in complex biofilm growth as that occurring in PUR supports [41]. The common practice is to calculate elemental sulfur production based on mass balances between the sulfide removed and the sulfate produced [32, 42-43] , which cannot be measured either. Developing monitoring tools and methods for obtaining additional data from biofilms is warranted for improving our modeling approach and to gain knowledge and robustness in the models proposed [44]. Such data together with a classical sensitivity analysis [45] would also contribute to reduce uncertainty of model parameters estimation. In fact, no work in literature has attempted to analyze neither the structural nor the parameter identifiabilities [46] of biofiltration models. It is well-known that modeling of biofiltration systems is based on models with a large number of parameters and processes that may be correlated which, coupled to a common lack of data of the biofilm (biofilm composition and structure, concentration of species in the biofilm…), lead to solutions that are fairly recognized as non-unique. However, the lack of such analysis/data and parameter correlation do not invalidate modeling efforts.

5. CONCLUSIONS

In this study heterogeneous respirometry was successfully applied to characterize the basic biofiltration properties (i.e. transport and biological phenomena) using a small and representative piece of packing material from an operating biotrickling filter in a short period of time, which allowed considering the biofilm properties as constant. Evaluation of mass transport by mimicking the hydraulic conditions of a BTF during the respirometric assays allowed estimating the contribution of wetted and non-wetted biofilms fractions to the overall removal of H_2S as well as to determine the limiting step. Then intrinsic biokinetic parameters were estimated with the minimal handling of the biofilm. This technique has shown to be highly adequate to study the kinetics of immobilized biomass which is essential in those generic models describing biofiltration process or other similar process involving biofilms. However, more data is needed, particularly from substrate degradation and inside the biofilm, to reduce uncertainty of model parameters estimation as well as to verify model predictions.

LIST OF SYMBOLS

a_{g-b} = gas-biofilm specific surface area, $m^2\ m^{-3}$

a_{g-l} = gas-liquid specific surface area, $m^2\ m^{-3}$

a_{l-b} = liquid-biofilm specific surface area, $m^2\ m^{-3}$

$C_{g,i}^{Bed}$ = concentration of component *i* in the gas phase in the bed, $g\ m^{-3}$

$C_{g,i}^{Free}$ = concentration of component *i* in the gas phase in the free section, $g\ m^{-3}$

$C_{l,i}^{Bed}$ = concentrations of component *i* in the liquid phase in the bed, $g\ m^{-3}$

$C_{l,i}^{Res}$ = concentrations of component *i* in the liquid phase in the reservoir section, g m^{-3}

$D_{eff,i}$ = diffusion coefficient of component *i* in the biofilm, m^2 h^{-1}

EC = elimination capacity, g m^{-3} h-1

He_i = gas/liquid partition coefficient of component *i* in a air/aqueous system

K_B = the external mass transfer coefficient from external bulk phase to biofilm, m h^{-1}

$K_L a_{g-l}$ = global mass transfer coefficient, h^{-1}

k_i = saturation constant for component *i*, g m^{-3}

$K_{s,i}$ = half saturation constant for component *i*, g m^{-3}

N = total number of layers that thickness biofilm was divided for the numerical resolution of the mathematical model

OUR = oxygen uptake rate, g O_2 m^{-3} h^{-1}

OUR_{max} = maximum oxygen uptake rate, g O_2 m^{-3} h^{-1}

OUR_{end} = endogenous oxygen uptake rate, g O_2 m^{-3} h^{-1}

Q_g = gaseous volumetric flow rate, m^3 h^{-1}

Q_l = liquid volumetric flow rate, m^3 h^{-1}

$r_{b,i}$ = consumption rates of component *i* in the wetted biofilm, g m^{-3} h^{-1}

$r_{b-NW,i}$ = consumption rates of component *i* in the non-wetted biofilm, g m^{-3} h^{-1}

t = time, h

t_{end}= final time of respirometry assay, h

t_{max}= time when maximum elimination capacity occurred, h

V_{bed}= packed bedvolume, m^3

V_{bio} = biomass volume, m^3

V_g = gaseous volume, m^3

V_l = liquid volume, m^3

x = thickness position in the biofilm, m

$Y_{O2/H2S}$ = yield coefficient, mol O_2 mol^{-1} H_2S

Subscripts

b = section of biofilm wetted

b-NW= section of biofilm non-wetted

i = component *i*

max = maximum

Superscripts

Bed = packed bed of HR

Free = gas free volume

Res = reservoir liquid volume

Greek Letters

α = surface fraction of packing material wetted

β= surface fraction of the packing material covered by biofilm

δ= biofilm thickness, m

ε_l^{Bed} = volume fraction occupied by the liquid in the packed bed, $m^3\ m^{-3}$

ε_g^{Bed} = volume fraction occupied by the gas in the packed bed, $m^3\ m^{-3}$

ε_b^{Bed} = volume fraction occupied by the biofilm in the packed bed, $m^3\ m^{-3}$

Acknowledgements

The Spanish government (MEC) provided financial support through the project CTM2009-14338-C03-01 and CTM2012-37927-C03-01. The Department of Chemical Engineering at UAB (Universitat Autònoma de Barcelona) is a unit of Biochemical Engineering of the Xarxa de Referència en Biotecnologia de Catalunya (XRB), Generalitat de Catalunya. The financial support of National Council of Science and Technology of Mexico CONACyT (CB-2011/168288) is also gratefully acknowledged.

REFERENCES

[1] N. Abatzoglou, S. Boivin, A review of biogas purification processes, Biofuels Bioprod. Biorefining, 3 (2009) 42-71.

[2] E. Ryckebosch, M. Drouillon, H. Veruaeren, Techniques for transformation of biogas to biomethane, Biomass Bioenerg., 35 (2011) 1633-1645.

[3] H.H.J. Cox, M.A. Deshusses, Biological waste air treatment in biotrickling filters, Curr. Opin. Biotechnol., 9 (1998) 256-262.

[4] M. Fortuny, J.A. Baeza, X. Gamisans, C. Casas, J. Lafuente, M.A. Deshusses, D. Gabriel, Biological sweetening of energy gases mimics in biotrickling filters, Chemosphere, 71 (2008) 10-17.

[5] S. Kim, M.A. Deshusses, Development and experimental validation of a conceptual model for biotrickling filtration of H_2S, Environ. Prog., 22 (2003) 119-128.

[6] H. Spanjers, P. Vanrolleghem, Respirometry as a tool for rapid characterization of wastewater and activated sludge, Water Sci. Technol., 31 (1995) 105-114.

[7] P.A. Vanrolleghem, H. Spanjers, B. Petersen, P. Ginestet, I. Takacs, Estimating (combinations of) Activated Sludge Model No. 1 parameters and components by respirometry, Water Sci. Technol., 39 (1999) 195-214.

[8] A.K. Gernaey, B. Petersen, J.P. Ottoy, P. Vanrolleghem, Activated sludge monitoring with combined respirometric-titrimetric measurements, Water Res., 35 (2001) 1280-1294.

[9] A. Guisasola, M. Pijuan, J.A. Baeza, J. Carrera, C. Casas, J. Lafuente, Aerobic phosphorus release linked to acetate uptake in bio-P sludge: Process modeling using oxygen uptake rate, Biotechnol. Bioeng., 85 (2004) 722-733.

[10] I. Garcia-Pena, S. Hernandez, R. Auria, S. Revah, Correlation of biological activity and reactor performance in biofiltration of toluene with the fungus *Paecilomyces variotii* CBS115145, Appl. Environ. Microbiol., 71 (2005) 4280-4285.

[11] R. Govind, W. Zhao, D.F. Bishop, Biofiltration kinetics for volatile organic compounds (VOCs) and development of a structure-biodegradability relationship, in: 90^{th} Annual Meeting and Exhibition of the Air and Waste Management Association, Pittsburg, PA, USA, 1997.

[12] R. Ramirez-Vargas, A. Ordaz, M. Carrion, I.Y. Hernandez-Paniagua, F. Thalasso, Comparison of static and dynamic respirometry for the determination of stoichiometric and kinetic parameters of a nitrifying process, Biodegradation, 24 (2013) 675-684.

[13] M. Piculell, T. Welander, K. Jonsson, Organic removal activity in biofilm and suspended biomass fractions of MBBR systems, Water Sci. Technol., 69 (2014) 55-61.

[14] A.M. Montebello, M. Fernandez, F. Almenglo, M. Ramirez, D. Cantero, M. Baeza, D. Gabriel, Simultaneous methylmercaptan and hydrogen sulfide removal in the desulfurization of biogas in aerobic and anoxic biotrickling filters, Chem. Eng. J., 200 (2012) 237-246.

[15] J.B.M. Klok, P.L.F. van den Bosch, C.J.N. Buisman, A.J.M. Stams, K.J. Keesman, A.J.H. Janssen, Pathways of sulfide oxidation by haloalkaliphilic bacteria in limited-oxygen gas lift bioreactors, Environ. Sci. Technol., 46 (2012) 7581-7586.

[16] D. Green, R. Perry, Perry's Chemical Engineers' Handbook, Mc. Graw-Hill, New York, 2007.

[17] V. Lazarova, J. Manem, Biofilm characterization and activity analysis in water and wastewater treatment, Water Res., 29 (1995) 2227-2245.

[18] W.C. Hugler, J. Cantu-De la Garza, M. Villa-Garcia, Biofilm analysis from an odor-removing trickling filter, in: 89th Annual Meeting and Exhibition of the Air and Waste Management Association, Pittsburg, PA, USA, 1996.

[19] A. Gonzalez-Sanchez, L. Arellano-Garcia, W. Bonilla-Blancas, G. Baquerizo, S. Hernandez, D. Gabriel, S. Revah, Kinetic characterization by respirometry of VOC-degrading biofilms from gas-phase biological filters, Ind. Eng. Chem. Res., (2014) Accepted.

[20] A. Gonzalez-Sanchez, G. Baquerizo, X. Gamisans, J. Lafuente, D. Gabriel, Short term characterization of a H_2S biotrickling filter packing using a gaseous-liquid respirometer, in: 3rd International Congress on Biotechniques for Air Pollution 2009, pp. 255-260.

[21] S. Kim, M.A. Deshusses, Determination of mass transfer coefficients for packing materials used in biofilters and biotrickling filters for air pollution control - 2: Development of mass transfer coefficients correlations, Chem. Eng. Sci., 63 (2008) 856-861.

[22] A.D. Dorado, F.J. Lafuente, D. Gabriel, X. Gamisans, A comparative study based on physical characteristics of suitable packing materials in biofiltration, Environ. Technol., 31 (2010) 193-204.

[23] A. Gonzalez-Sanchez, M. Tomas, A.D. Dorado, X. Gamisans, A. Guisasola, J. Lafuente, D. Gabriel, Development of a kinetic model for elemental sulfur and sulfate formation from the autotrophic sulfide oxidation using respirometric techniques, Water Sci. Technol., 59 (2009) 1323-1329.

[24] C.J. Mpanias, B.C. Baltzis, An experimental and modeling study on the removal of mono-chlorobenzene vapor in biotrickling filters, Biotechnol. Bioeng., 59 (1998) 328-343.

[25] B.C. Baltzis, C.J. Mpanias, S. Bhattacharya, Modeling the removal of VOC mixtures in biotrickling filters, Biotechnol. Bioeng., 72 (2001) 389-401.

[26] H. Li, J.C. Crittenden, J.R. Mihelcic, H. Hautakangas, Optimization of biofiltration for odor control: model development and parameter sensitivity, Water Environ. Res., (2002) 5-16.

[27] A. Gonzalez-Sanchez, S. Revah, The effect of chemical oxidation on the biological sulfide oxidation by an alkaliphilic sulfoxidizing bacterial consortium, Enzyme Microbiol. Technol., 40 (2007) 292-298.

[28] S. Kim, M.A. Deshusses, Understanding the limits of H_2S degrading biotrickling filters using a differential biotrickling filter, Chem. Eng. J., 113 (2005) 119-126.

[29] S. Kim, M.A. Deshusses, Determination of mass transfer coefficients for packing materials used in biofilters and biotrickling filters for air pollution control. 1. Experimental results, Chem. Eng. Sci., 63 (2008) 841-855.
[30] N. Abdehagh, M.T. Namini, B. Bonakdarpour, S.M. Heydarian, Effect of operating parameters on the performance of a *Thiobacillus thioparus*-immobilized polyurethane foam biotrickling filter for hydrogen sulfide removal, Clean-Soil Air Water, 42 (2014) 1311-1317.
[31] A. Tamimi, E.B. Rinker, O.C. Sandall, Diffusion coefficients for hydrogen sulfide, carbon dioxide, and nitrous oxide in water over the temperature range 293-368-K, J. Chem. Eng. Data, 39 (1994) 330-332.
[32] M. Ramirez, J.M. Gomez, G. Aroca, D. Cantero, Removal of hydrogen sulfide by immobilized Thiobacillus thioparus in a biotrickling filter packed with polyurethane foam, Biores. Technol., 100 (2009) 4989-4995.
[33] G. Rodriguez, A.D. Dorado, A. Bonsfills, R. Sanahuja, D. Gabriel, X. Gamisans, Optimization of oxygen transfer through venturi-based systems applied to the biological sweetening of biogas, J. Chem. Technol. Biotechnol., 87 (2012) 854-860.
[34] A.M. Montebello, M. Mora, L.R. López, T. Bezerra, X. Gamisans, J. Lafuente, M. Baeza, D. Gabriel, Aerobic desulfurization of biogas by acidic biotrickling filtration in a randomly packed reactor, J. Hazard. Mater., 280 (2014) 200-208.
[35] M. Tomàs, M. Fortuny, C. Lao, D. Gabriel, J. Lafuente, X. Gamisans, Technical and economical study of a full-scale biotrickling filter for H_2S removal from biogas, Water Pract. Technol., 4 (2009).
[36] M. Fortuny, A. Guisasola, C. Casas, X. Gamisans, J. Lafuente, D. Gabriel, Oxidation of biologically produced elemental sulfur under neutrophilic conditions, J. Chem. Technol. Biotechnol., 85 (2010) 378-386.
[37] G. Trejo-Aguilar, S. Revah, R. Lobo-Oehmichen, Hydrodynamic characterization of a trickle bed air biofilter, Chem. Eng. J., 113 (2005) 145-152.
[38] J. Silva, M. Morales, M. Caceres, P. Morales, G. Aroca, Modelling of the biofiltration of reduced sulphur compounds through biotrickling filters connected in series: Effect of H_2S, Electron. J. Biotechnol., 15 (2012).
[39] A.K. Dhussa, S.S. Sambi, S. Kumar, S. Kumar, J.K. Prajapati, Simplified simulation model of a biotrickling filter used for the removal of hydrogen sulfide from biogas, Int. J. Chem. React. Eng., 10 (2012).
[40] R. Lebrero, J.M. Estrada, R. Munoz, G. Quijano, Toluene mass transfer characterization in a biotrickling filter, Biochem. Eng. J., 60 (2012) 44-49.
[41] L. Arellano-García, A. D.Dorado, A. Morales-Guadarrama, , E. Sacristan, X. Gamisans, S. Revah, Modeling the effects of biomass accumulation on the performance of a biotrickling filter packed with PUF support for the alkaline biotreatment of dimethyl disulfide vapors in air. Appl. Microbiol. Biotechnol., 99 (2015) 97-107.

[42] R.B. Solcia, M. Ramirez, M. Fernandez, D. Cantero, D. Bevilaqua, Hydrogen sulphide removal from air by biotrickling filter using open-pore polyurethane foam as a carrier, Biochem. Eng. J., 84 (2014) 1-8.
[43] Y.M. Jin, M.C. Veiga, C. Kennes, Effects of pH, CO2, and flow pattern on the autotrophic degradation of hydrogen sulfide in a biotrickling filter, Biotechnol. Bioeng., 92 (2005) 462-471.
[44] X. Guimerà, A. Moya, A. Dorado, R. Villa, D. Gabriel, G. Gabriel, X. Gamisans, Biofilm dynamics characterization using a novel DO-MEA sensor: mass transport and biokinetics, Appl. Microbiol. Biotechnol., (2014) 1-12.
[45] G. Baquerizo, J.P. Maestre, T. Sakuma, M.A. Deshusses, X. Gamisans, D. Gabriel, J. Lafuente, A detailed-model of a biofilter for ammonia removal: Model parameters analysis and model validation, Chem. Eng. J., 113 (2005) 205-214.
[46] B. Petersen, K. Gernaey, M. Devisscher, D. Dochain, P.A. Vanrolleghem, A simplified method to assess structurally identifiable parameters in Monod-based activated sludge models, Water Res., 37 (2003) 2893-2904.

FIGURE CAPTIONS

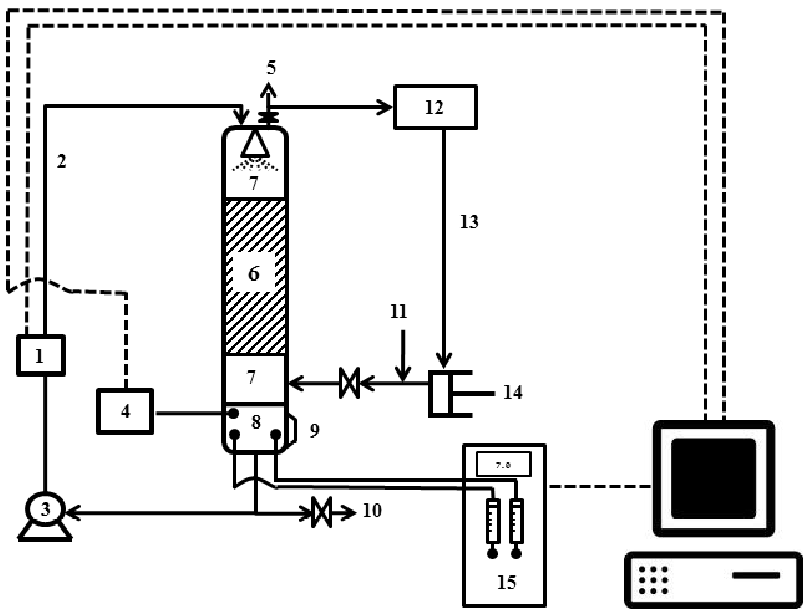

Fig. 1. Schematic of the Heterogeneous Respirometer. (1) dissolved oxygen sensor, (2) liquid recirculation, (3) Liquid recirculation pump, (4) pH sensor, (5) Gas out, (6) Packed bed, (7) Gas free (gas volume out of the packed bed), (8) Liquid reservoir, (9) Pulse port, (10) Liquid purge, (11) Gas in, (12) O_2/CO_2 sensor , (13) Gas recirculation, (14) Gas recirculation compressor, (15) micro-burette for pH control.

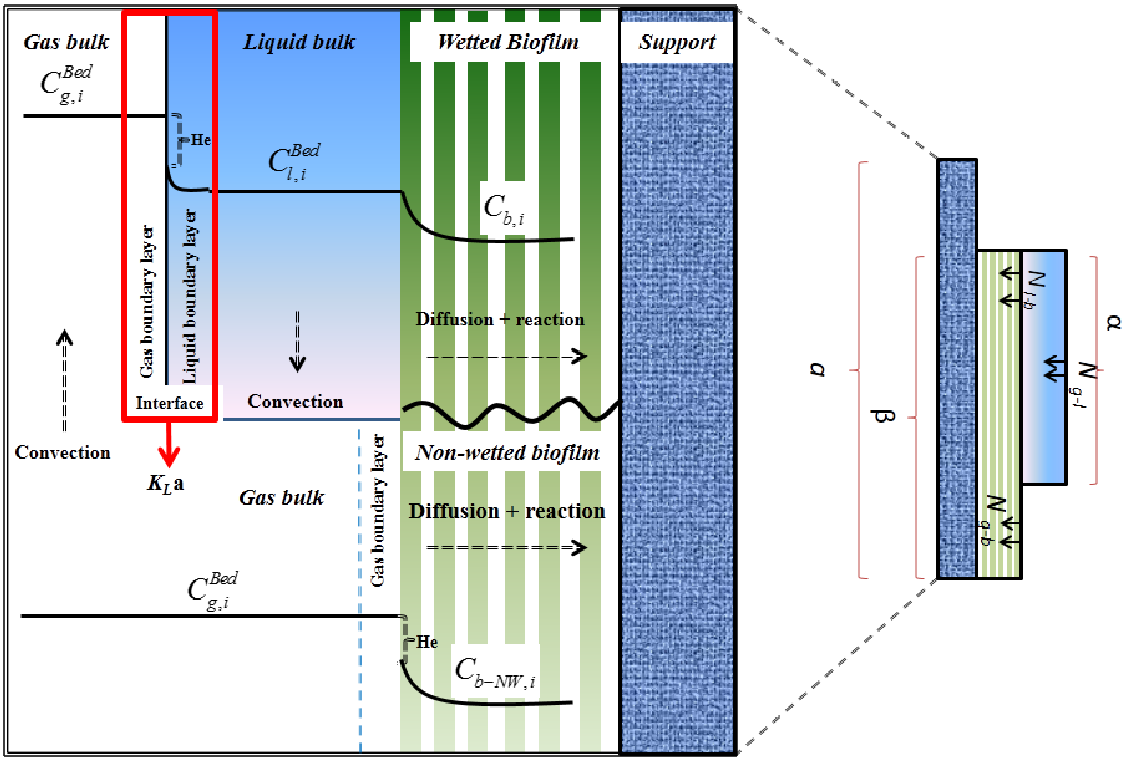

Fig. 2. Schematic of the phenomena and mechanisms of the H_2S removal in a biotrickling filter, assuming wetted and non-wetted biofilm. $N_{l\text{-}b}$, $N_{g\text{-}l}$, $N_{g\text{-}b}$ refer to mass fluxes between phases.

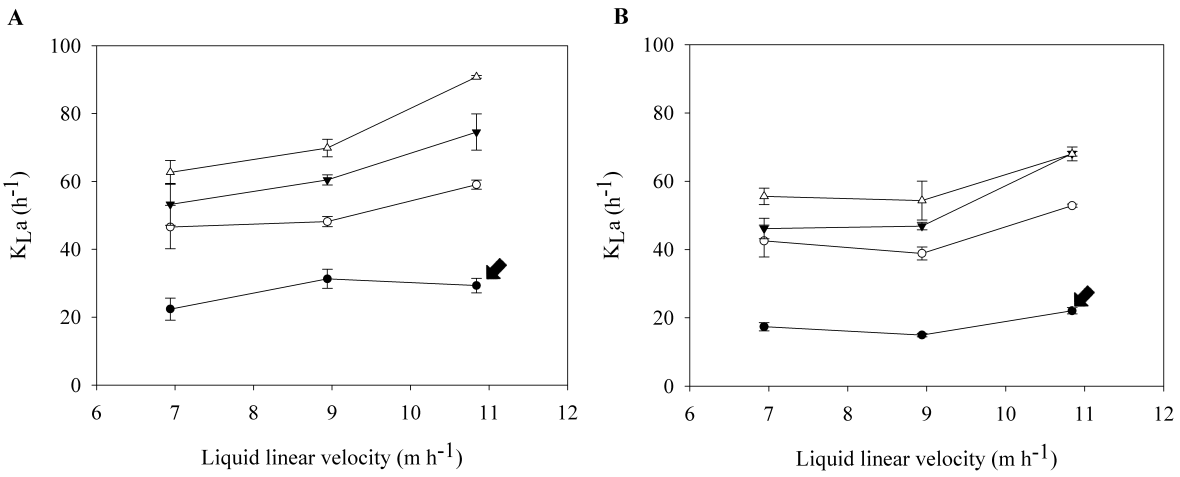

Fig. 3. Mass transfer coefficient for the two different packing materials tested at different gas and liquid flow rates. A) Stainless steel PR, B) PUF: Gas velocity 43.37 m h^{-1} (●) Gas velocity 57.83 m h^{-1} (○), Gas velocity 77.11 m h^{-1} (▼), Gas velocity 101.21 m h^{-1} (△). Values marked with an arrow indicate the values used for biotic tests.

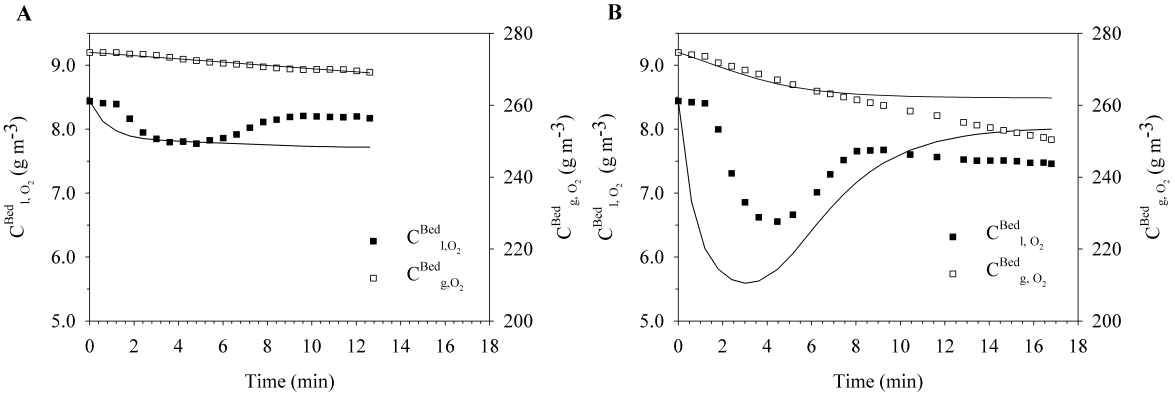

Fig. 4. Experimental results and predicted profiles of the HR model obtained from the respirometric assays with a gas pulse of 10 mL of pure H_2S: Gas-experimental (□), Gas-model (--), Liquid-experimental (■), Liquid-Model (-). A) Stainless steel PR, B) PUF.

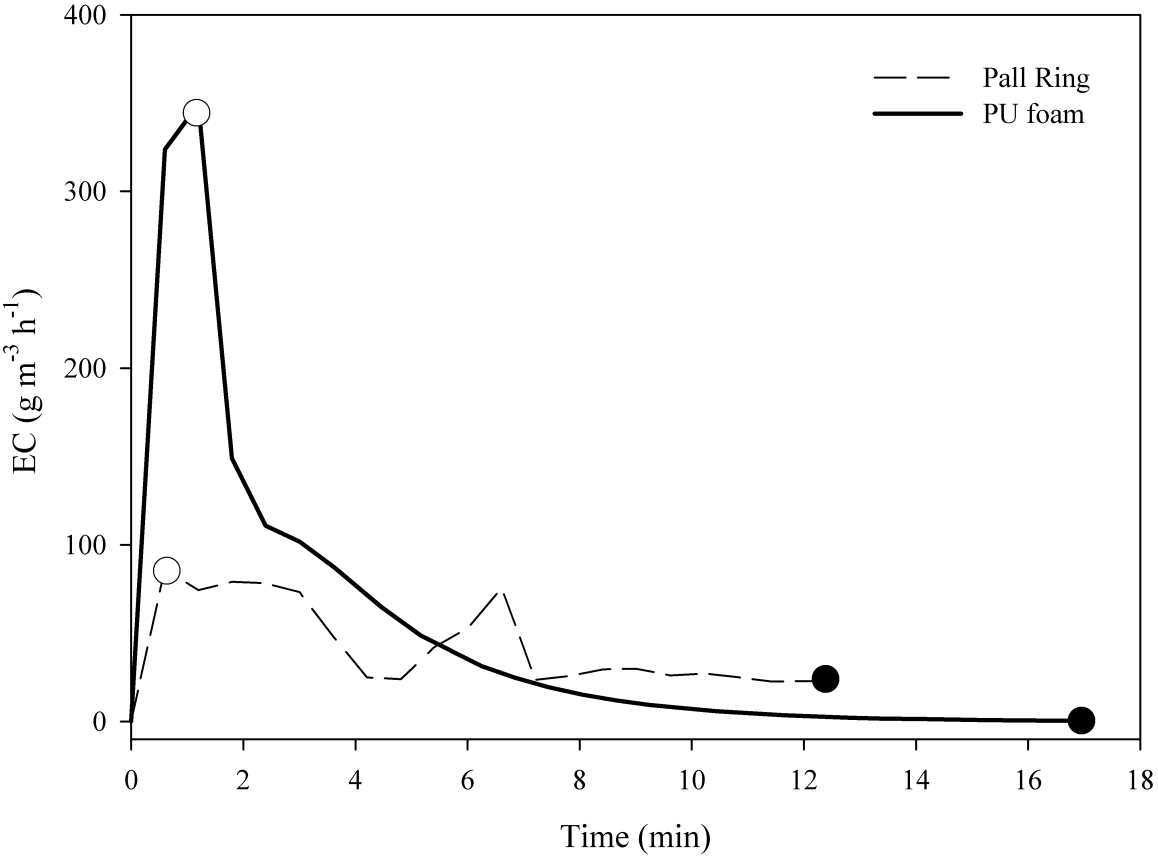

Fig. 5. Predicted H_2S elimination capacity for the wetted and non-wetted fractions of colonized PUF and PR packing materials. Circles indicate the time at which the rate controlling step was assessed: t_{max}, (○) and t_{end} (●).

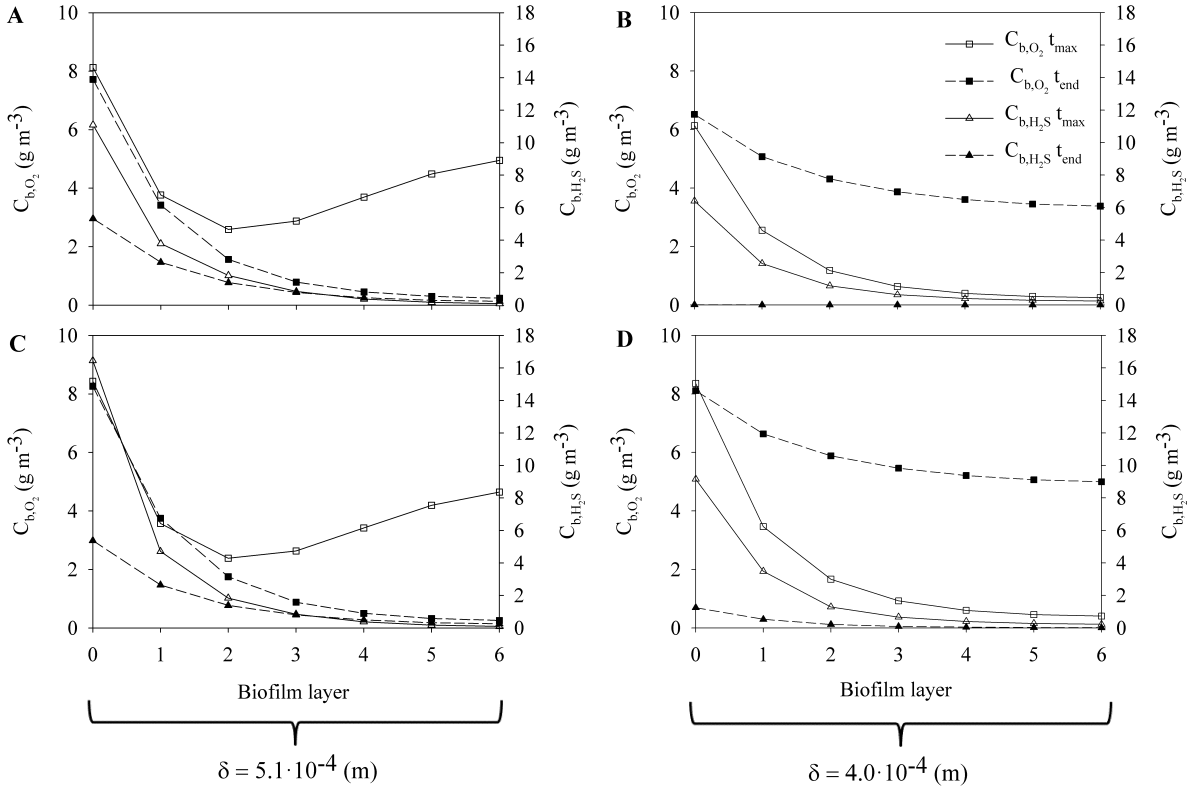

Fig. 6. Simulated dissolved H_2S and oxygen concentration profiles inside the biofilm, at t_{max} and t_{end} for A) wetted stainless steel PR, B) wetted PUF, C) non-wetted stainless steel PR, and D) non-wetted PUF.

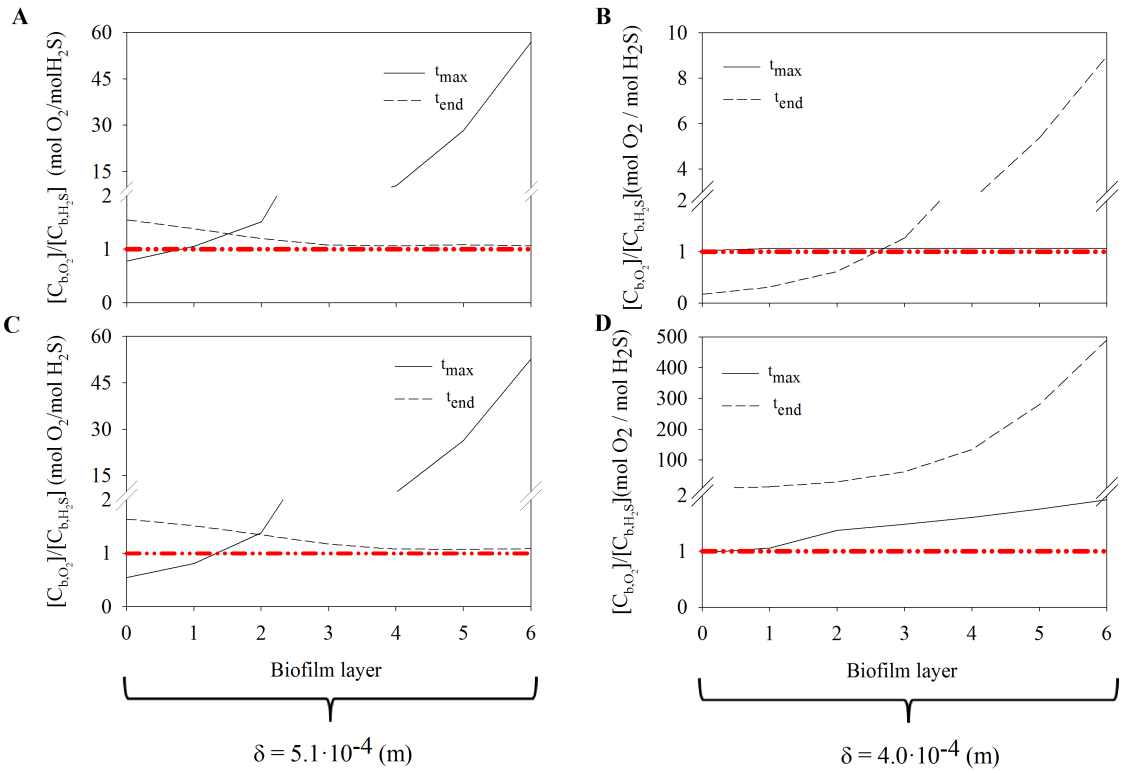

Fig. 7. Dissolved oxygen and H_2S concentrations ratios inside the biofilm at t_{max} and t_{end} for A) wetted stainless steel PR, B) wetted PUF, C) non-wetted stainless steel PR, and D) non-wetted PUF. Dash-dotted lines correspond to the molar ratio at which stoichiometry switches occur.

1

Table 1. Parameters included in the mathematical model

	Colonized Pall Rings		Colonized Polyurethane Foam		
Parameter	**Value**	**Ref.**	**Value**	**Ref.**	**Units**
ε_g	0.70	E.D.	0.85	E.D.	$m^3_{gas} \cdot m^{-3}_{bed}$
ε_b	0.06	E.D.	0.21	E.D.	$m^3_{biofilm}\ m^{-3}_{bed}$
ε_l	0.10	E.D.	0.09	E.D.	$m^3_{liquid}\ m^{-3}_{bed}$
ε_S	0.18	M.D.	0.03	M.D.	$m^3_{liquid}\ m^{-3}_{bed}$
a	482.00	M.D.	600.00	M.D.	$m^2\ m^{-3}_{bed}$
$Ks_{,O2}$	1.47	[19]	1.47	[19]	$g\ m^{-3}$
$\mathcal{D}_{iff_{O_2}}$	$7.10x10^{-6}$	ICAS[a]	$7.10x10^{-6}$	ICAS[a]	$m^2\ h^{-1}$
$\mathcal{D}_{iff_{H_2S}}$	$6.30x10^{-6}$	[31]	$6.30x10^{-6}$	[31]	$m^2\ h^{-1}$
He_{O2}	32.60	ICAS[a]	32.60	ICAS[a]	
He_{H2S}	0.41	[16]	0.41	[16]	
$K_L a_{g\text{-}l}$	29.31±2.1	E.D.	22.08±0.9	E.D.	h^{-1}
$V_{g\ res}$	$6.30x10^{-4}$	E.D.	$6.30x10^{-4}$	E.D.	m^3
$V_{l\ res}$	$1.26x10^{-4}$	E.D.	$1.26x10^{-4}$	E.D.	m^3
V_{bed}	$6.10x10^{-4}$	E.D.	$6.10x10^{-4}$	E.D.	m^3
α	0.38	[5]	0.36	[5]	$m^2_{liquid}\ m^{-2}_{bed}$
OUR_{end}	6.00	E.D.	7.00	E.D.	$g\ O_2\ m^{-3}$ biomass h^{-1}

[a]*ICAS 13 data base, Denmark.*
E.D. Experimental determination.
M.D. Manufacturer data

2

Table 2 Fitted parameters for the calibration of the HR mathematical model to the respective PR and PUF assays and other relevant parameters computed.

Parameter	Colonized Pall Rings	Colonized Polyurethane Foam	**Units**
OUR_{max} (best fitted)	16237.0	27202.4	g O_2 m^{-3} biomass h^{-1}
δ (best fitted)	5.1 x 10^{-4}	4.0 x 10^{-4}	m
$Ks_{,H2S}$ (best fitted)	9.9	9.9	g m^{-3}
Ki (best fitted)	69.7	69.5	g m^{-3}
EC_{max}	85.7	349.4	g H_2S m^{-3} h^{-1}
β	0.2	0.8	m^2 bio m^{-2} bed
$q\ O_{2\ max}$	23.0	38.55	mmol O_2 (g biomass min)$^{-1}$
a_{l-b}	44.7	180.0	m^2 wetted biofilm m^{-3} bed
a_{g-b}	72.9	320.0	m^2 non-wetted biofilm m^{-3} bed